Cell, Vol. 107, 399–407, November 2, 2001, Copyright ©2001 by Cell Press

Crystal Structure of a Procaspase-7 Zymogen: Mechanisms of Activation and Substrate Binding

Jijie Chai,[1] Qi Wu,[1] Eric Shiozaki,[1] Srinivasa M. Srinivasula,[2] Emad S. Alnemri,[2] and Yigong Shi[1,3]

[1] Department of Molecular Biology
Lewis Thomas Laboratory
Princeton University
Princeton, New Jersey 08544

[2] Kimmel Cancer Center
233 South 10th Street
Thomas Jefferson University
Philadelphia, Pennsylvania 19107

Summary

Apoptosis is primarily executed by active caspases, which are derived from the inactive procaspase zymogens through proteolytic cleavage. Here we report the crystal structures of a caspase zymogen, procaspase-7, and an active caspase-7 without any bound inhibitors. Compared to the inhibitor-bound caspase-7, procaspase-7 zymogen exhibits significant structural differences surrounding the catalytic cleft, which precludes the formation of a productive conformation. Proteolytic cleavage between the large and small subunits allows rearrangement of essential loops in the active site, priming active caspase-7 for inhibitor/substrate binding. Strikingly, binding by inhibitors causes a 180° flipping of the N terminus in the small subunit, which interacts with and stabilizes the catalytic cleft. These analyses reveal the structural mechanisms of caspase activation and demonstrate that the inhibitor/substrate binding is a process of induced fit.

Introduction

Apoptosis plays an essential role in the development of all multicellular organisms and the homeostasis of adult tissues (Horvitz, 1999; Jacobson et al., 1997; Steller, 1995). Alterations in apoptotic pathways have been implicated in many diseases, such as cancer and neurodegenerative disorders (Thompson, 1995; Yuan and Yankner, 2000). The mechanism of apoptosis is remarkably conserved across species, executed with a cascade of sequential activation of initiator and effector caspases (Budihardjo et al., 1999; Thornberry and Lazebnik, 1998).

Caspases are a family of *c*ysteine proteases that cleave their substrates after an *asp*artate residue. Since the discovery of caspase-1 (also known as interleukin 1β-converting enzyme or ICE) (Cerreti et al., 1992; Thornberry et al., 1992), 13 others have been reported, of which at least eight are involved in programmed cell death. All caspases are produced in cells as catalytically inactive zymogens and must be proteolytically processed to become active proteases. The activation of an effector caspase, such as caspase-7, is performed by an initiator caspase, such as caspase-9, through proteolytic cleavage at specific internal Asp residues to separate the large and small subunits of the mature caspase (Srinivasula et al., 1998a). Once activated, the effector caspases are responsible for the proteolytic degradation of a broad spectrum of cellular targets, leading ultimately to cell death (Thornberry and Lazebnik, 1998). Among the effector caspases, caspase-7 shares 54% sequence identity with caspase-3 (Fernandes-Alnemri et al., 1995); these two caspases exhibit highly similar structures and function.

Because the modulation of caspase activity could prove important for the therapeutic intervention of many diseases, structural characterization of caspases has been a center of focus in the apoptosis field (Shi, 2001). Structural information is now available on caspase-1 (Walker et al., 1994; Wilson et al., 1994), caspase-3 (Mittl et al., 1997; Rotonda et al., 1996), caspase-7 (Wei et al., 2000), and caspase-8 (Blanchard et al., 1999; Watt et al., 1999). Indeed, peptide-based inhibitors of caspases have shown efficacy in animal models of several clinical disorders, including stroke (Cheng et al., 1998; Endres et al., 1998), traumatic brain injury (Yakovlev et al., 1997), and fulminant liver destruction (Rodriguez et al., 1996). To improve the design and efficacy of potential drugs, it is important to understand the fundamental mechanisms of caspase activation and substrate/inhibitor binding.

However, despite intense effort, all reported structural information on caspases to date is restricted to caspases bound with designed or natural inhibitors (Chai et al., 2001; Huang et al., 2001; Riedl et al., 2001). In particular, there is no structural information on any procaspase zymogen or any active caspase without bound cofactors. Consequently, it is entirely unknown how procaspase zymogens are activated and what structural changes are associated with the interdomain cleavage. In addition, although the catalytic pocket is highly similar in reported caspase structures, it is unclear whether this rigid conformation is preformed or induced by inhibitor binding. This distinction is particularly important for the discovery of potent caspase inhibitors.

To understand the fundamental mechanisms of caspase activation and substrate/inhibitor binding, we determined the crystal structures of an unprocessed procaspase-7 zymogen and a processed active caspase-7. These structures reveal large conformational changes associated with the interdomain cleavage, and, in conjunction with the structure of caspase-7 bound to an inhibitor (Chai et al., 2001; Huang et al., 2001; Wei et al., 2000), provide a structural mechanism for caspase activation and substrate/inhibitor binding. This mechanism explains a body of published evidence and serves as a general framework for understanding caspases.

Results

Structure of an Unprocessed Procaspase-7 Zymogen

The full-length procaspase-7 zymogen contains 303 amino acids. When overexpressed in bacteria, autocata-

[3] Correspondence: yshi@molbio.princeton.edu

Table 1. Data Collection and Statistics from the Crystallographic Analysis

Data set	Procaspase-7 (NSLS-X25)	Caspase-7 (NSLS-X25)
Spacegroup	$P3_221$	$P3_221$
Resolution (Å)	99.0–2.70	99.0–2.60
Total observations	97,318	150,937
Unique observations	21,329	23,466
Data coverage	90.9%	89.2%
R_{sym} (outer shell)	0.048 (0.270)	0.061 (0.180)
Refinement		
Resolution range (Å)	20–2.70	20–2.60
Number of reflections ($I > 0.5\sigma$)	20,735	22,194
$R_{working}/R_{free}$	22.7%/25.3%	23.2%/25.7%
Number of atoms	3,692	3,706
Number of waters	82	49
Rmsd bond length (Å)	0.008	0.009
Rmsd bond angles (degree)	1.62	2.12

$R_{sym} = \Sigma_h\Sigma_i \mid I_{h,i} - I_h \mid / \Sigma_h\Sigma_i I_{h,i}$, where I_h is the mean intensity of the i observations of symmetry related reflections of h. $R = \Sigma \mid F_{obs} - F_{calc} \mid / \Sigma F_{obs}$, where $F_{obs} = F_P$, and F_{calc} is the calculated protein structure factor from the atomic model (R_{free} was calculated with 5% of the reflections). Rmsd in bond lengths and angles are the deviations from ideal values, and the rmsd deviation in B factors is calculated betwen bonded atoms.

lytic cleavage after Asp198 gives rise to a fully active caspase-7. To prevent this proteolytic activation, we mutated the catalytic residue Cys186 to Ala. This procaspase-7 variant (C186A) was expressed as a single contiguous polypeptide, purified to homogeneity, and crystallized. The structure was determined by molecular replacement and refined at 2.7 Å resolution with crystallographic working and free R factors of 22.7% and 25.3%, respectively (Table 1 and Figure 1).

Similar to the active caspase-7, the procaspase-7 zymogen comprises two catalytic units, each containing a central 6-stranded β sheet and five α helices (Figure 1A). Four surface loops (L1–L4) emanate from these core structural elements, forming a potential catalytic site. Compared to the inhibitor-bound caspase-7 (Chai et al., 2001), the core structural elements remain nearly identical, with less than 0.8 Å root-mean-square deviation (Rmsd) for all 360 aligned Cα atoms (Figure 1B). However, three of the four active site loops adopt drastically different conformations (Figures 1B and 1C). Loop L3, which forms the base of the catalytic groove in the active caspase-7, expands and moves out of the base (Figure 1C). Loop L4, which forms one side of the catalytic groove in the active caspase-7 (Chai et al., 2001; Huang et al., 2001), rotates 60° and moves in the opposite direction as L3, further flattening the active site pocket (Figure 1C). Most importantly, loop L2, which contains the catalytic residue Cys186, changes its direction by 90° and makes this residue inaccessible to solvent (Figure 1C). Among the four loops, only L1 retains its active site conformation (Figure 1C).

Compared to the catalytic groove in the active caspase-7 formed by the four loops (Figure 1D), these structural rearrangements in the procaspase-7 zymogen do not give rise to a recognizable substrate binding site (Figure 1E). In particular, loops L4, L2, and L2′ form a "loop-bundle" through numerous interactions in the inhibitor-bound caspase-7 (Chai et al., 2001; Huang et al., 2001) (Figures 1C and 2A). This loop-bundle stabilizes the conformation of the active site loop L2 as well as the overall shape and fold of the catalytic groove (Figure 2A). However, in the procaspase-7 zymogen, loop L2′ is flipped by 180°, disallowing the formation of this loop-bundle structure. These structural rearrangements explain why the procaspase-7 zymogen does not possess detectable catalytic activity.

The procaspase-7 zymogen is a single contiguous polypeptide chain, with loop L2 linking the large and the small subunits. This interdomain loop contains the cleavage site (Ile195-Gln196-Ala197-Asp198) for the activation of procaspase-7, which requires a certain degree of flexibility in this region for binding to the active sites. In the crystals, there was no clear electron density for part of the L2 loop (residues 190–203) that centers on the cleavage site, confirming that these regions are indeed highly flexible and disordered in solution (Figure 1A).

Each heterodimer of caspase-7 may be derived from the same polypeptide chain, or from two separate polypeptide chains as proposed by an interdigitating model. These two models cannot by distinguished by in vivo studies, as the presence of other caspases inevitably complicates interpretation of results. Recent in vitro studies indicate that each heterodimer of caspase-9 is derived from a single polypeptide (Srinivasula et al., 1998a). In the crystals, the N terminus of the small subunit in one heterodimer traverses along the interface between two heterodimers and comes close to the C terminus of the large subunit in the same heterodimer, as judged by electron density (Figure 1A). This arrangement supports the conclusion that each heterodimer results from the same polypeptide. Based on this observation, we term the two interdomain loops L2 and L2′, respectively (Figure 1A).

Structural Rearrangements in the Loop-Bundle

In the active caspase-7 bound with peptide inhibitors, the catalytic groove is well defined by four surrounding loops (Chai et al., 2001; Huang et al., 2001) (Figures 1B and 1C). The productive positioning of the catalytic residue Cys186 is facilitated by the extended conformation of the L2 loop (Figure 2A). The L2 loop, on the other

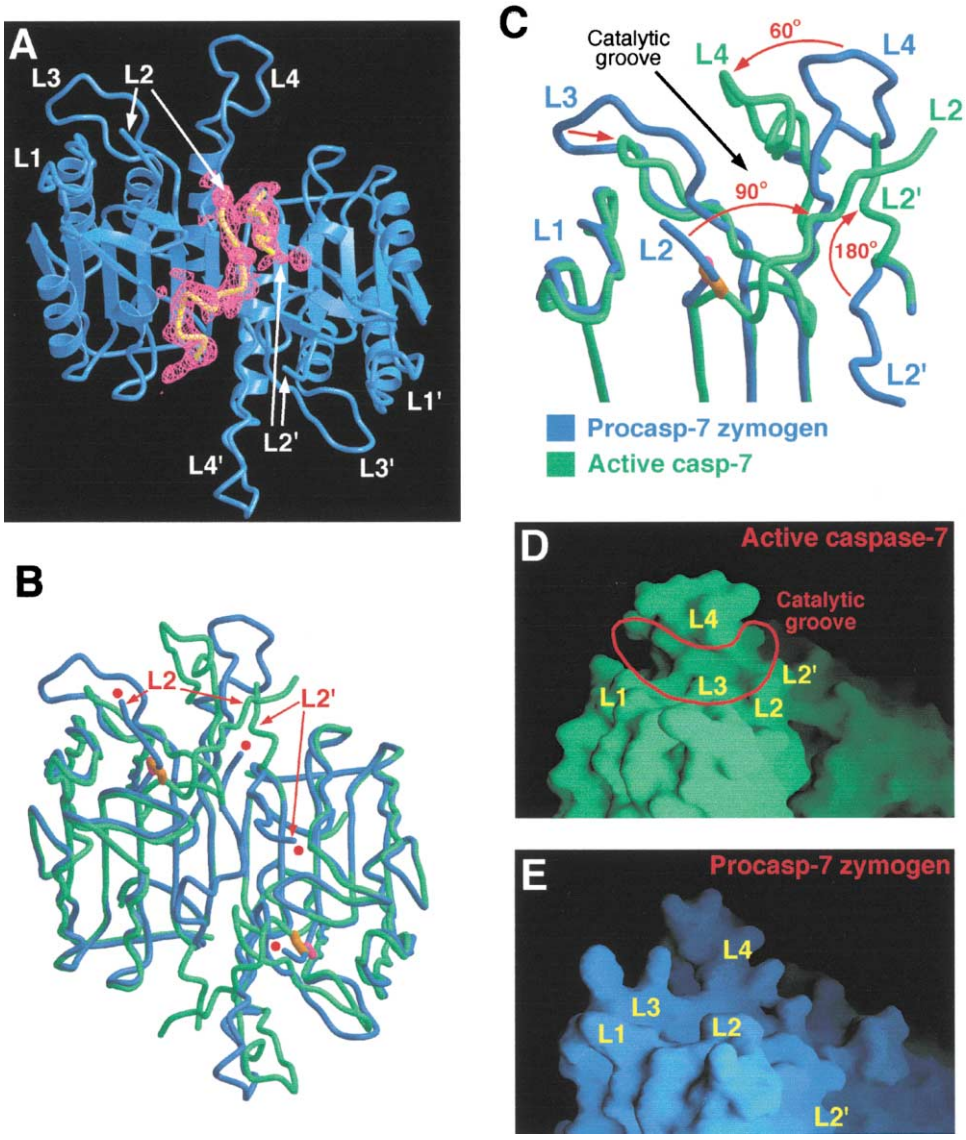

Figure 1. Structural Comparison of the Unprocessed Procaspase-7 Zymogen and the Active Caspase-7 Bound with an XIAP Fragment (PDB code 1I51)

(A) Overall structure of the procaspase-7 zymogen. The structure is shown in blue, with the N termini of the small subunits highlighted in yellow. The electron density (omit map) surrounding the N termini of the small subunits, shown at 2.5 σ, was calculated by simulated annealing using CNS (Brunger et al., 1998). The four loops that define the catalytic groove are labeled.

(B) Superposition of the unprocessed procaspase-7 zymogen (blue) with the active caspase-7 (green) bound with an XIAP fragment. For clarity, the XIAP fragment is not shown here. The open termini of the interdomain loops (L2 and L2′) in procaspase-7 are indicated by red dots. The residues between these termini are flexible and disordered in the crystals.

(C) Close-up comparison of the four loops that define the catalytic cleft. The arrows indicate structural changes from the procaspase-7 zymogen to the active caspase-7. The catalytic residue is colored gold and red, respectively, for the active caspase-7 and the zymogen. The orientation for procaspase-7 is the same for (A), (B), and (C).

(D) Surface representation of the catalytic groove in the active caspase-7 bound with an XIAP fragment. For an unobstructed view, the XIAP fragment is not shown.

(E) Surface representation of the corresponding region in the procaspase-7 zymogen. Note the disappearance of the catalytic groove. The procaspase-7 zymogen is shown in an identical orientation as the active caspase-7 (D). Figures 1, 2, and 4 were prepared using MOLSCRIPT (Klaulis, 1991) and GRASP (Nicholls et al., 1991).

hand, is involved in networks of contacts with the L4 and L2′ loops, forming the so-called loop-bundle (Figure 2A). There are a total of 11 hydrogen bonds and numerous van der Waals interactions in the loop-bundle region, centering on residues Asp192 of the L2 loop and Pro214 of the L2′ loop (Figure 2A). These interactions not only stabilize the L2 loop but also engage the L4 loop to maintain a productive conformation for the catalytic cleft to which the inhibitors/substrates bind.

In the procaspase-7 zymogen, the loop-bundle is completely dissolved (Figure 2B). Rather than engaging the N-terminal portions of loops L2 and L4, the N termi-

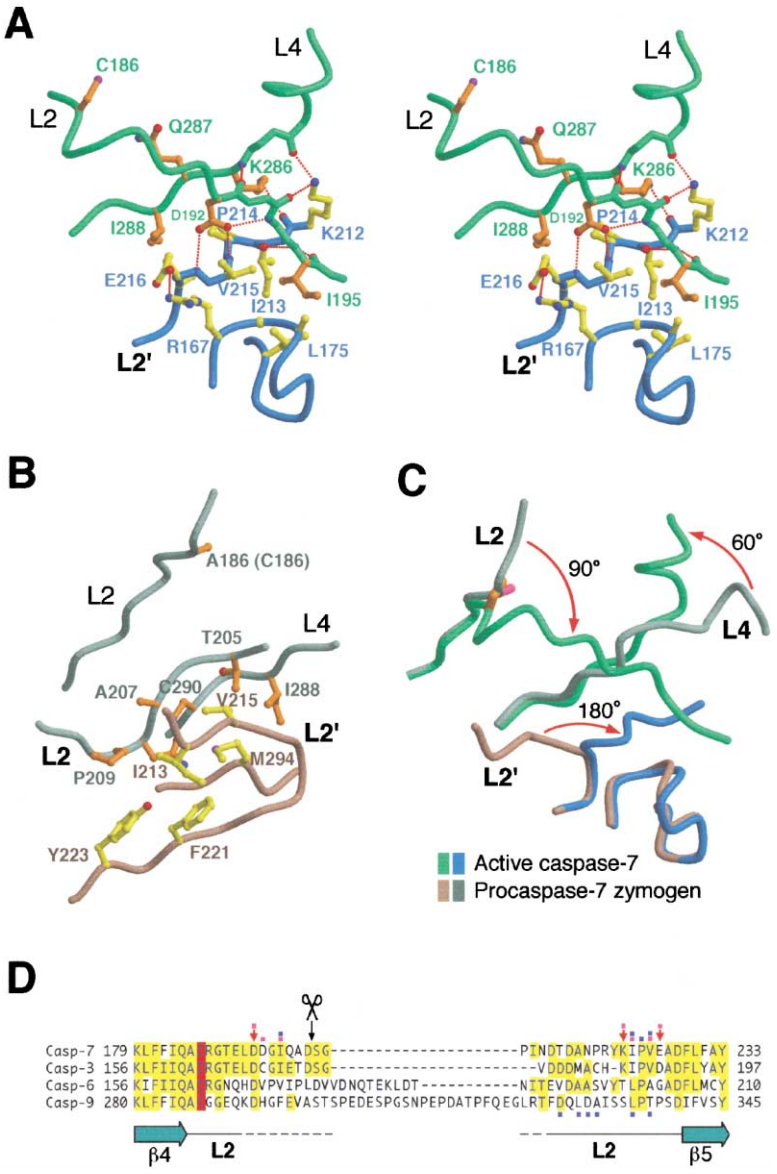

Figure 2. A Structural Mechanism for the Activation of Procaspase-7

(A) Stabilization of the catalytic cleft by the loop-bundle in the active caspase-7 bound with an XIAP fragment (PDB code 1I51). The loop-bundle is nucleated by the free N terminus (L2′) of the small subunit. These interactions occur between two adjacent caspase-7 heterodimers. Fragments from these two heterodimers are colored green and blue, respectively. Their side chains are colored gold and yellow, respectively. Hydrogen bonds are represented by red dashed lines.

(B) The uncleaved interdomain loop in the procaspase-7 zymogen is restrained to adopt a different set of interactions. Fragments from two adjacent heterodimers are colored gray and brown, respectively.

(C) Superposition of the loop-bundle in the active caspase-7 and the corresponding regions in the procaspase-7 zymogen. Coloring scheme is the same as in (A) and (B). The orientation of active caspase-7 is the same for (A) and (C). The orientation of procaspase-7 in this panel is highly similar (a rotation of 5° along vertical axis) to that in (B).

(D) Sequence alignment of the L2 loop region for caspase-3, -6, -7, and -9. The catalytic Cys is highlighted in red, while conserved residues are colored yellow. Interactions in the procaspase-7 zymogen and the XIAP-bound active caspase-7 are shown below and above the alignment, respectively. Residues that make hydrogen bonds in the loop-bundle region with their side chain and main chain groups are indicated by red arrows and red squares, respectively. Residues that make van der Waals contacts are identified by blue squares. The scissors indicate the position of activation cleavage in procaspase-7 and -3.

nus of the L2′ loop folds back to interact with the C-terminal portions of loops L2 and L4, existing in a "closed" conformation. These interactions, exclusively comprising van der Waals contacts (Figure 2B), appear to be weaker than those observed in the inhibitor-bound caspase-7 (Figure 2A).

Why is there such a drastic conformational change between the procaspase-7 zymogen and the inhibitor-bound caspase-7 (Figure 2C)? One essential reason resides in the unprocessed nature of the procaspase-7 zymogen. As the C-terminal portion of the loop L2′ is covalently connected to its N-terminal portion which resides near the catalytic site on the opposite end (Figure 1A), the L2′ loop is physically occluded from being able to form a loop-bundle with loops L2 and L4. This inability can only be removed by a proteolytic cleavage after Asp198, which allows the L2′ loop to switch to its open conformation as observed in the inhibitor-bound caspase-7 (Figure 2C).

Sequence alignment reveals that the two central residues in the loop-bundle, Asp192 on loop L2 and Pro214 on loop L2′, are invariant among caspases (Figure 2D). Other residues involved in stabilizing the loop-bundle in the inhibitor-bound caspase-7 and the corresponding region in the procaspase-7 zymogen are also generally conserved. These observations suggest that the activation mechanism observed for caspase-7 is likely true for other caspases such as caspase-3 and caspase-6. Supporting this analysis, the inhibitor-bound caspase-3 contains a highly similar loop-bundle that stabilizes the substrate-bound conformation (Mittl et al., 1997; Rotonda et al., 1996; Wei et al., 2000). Compared to caspase-7, caspase-9 contains an expanded L2 loop (Figure 2D), which may allow enough conformational flexibility such that caspase-9 does not need an interdomain cleavage to have the L2′ loop move to its productive conformation. This is consistent with the finding that procaspase-9 exhibits a basal level of activity in

the absence of any proteolytic cleavage (Srinivasula et al., 2001; Stennicke et al., 1999).

The N-Terminal Prodomain Is Dispensable for Caspase-7 Activity

In the crystals of the procaspase-7 zymogen, there is no electron density for the N-terminal prodomain sequences (residues 1–55), suggesting that these sequences are not necessary for the activation of procaspase-7 or the activity of mature caspase-7. Supporting this observation, a caspase-7 variant with the N-terminal 50 residues deleted is fully able to undergo autoactivation when overexpressed in bacteria (Chai et al., 2001). In addition, this variant, when purified to homogeneity, exhibits catalytic activity indistinguishable to that of the wild-type caspase-7 (data not shown). Furthermore, consistent with our structural observations, the presence or absence of the N-terminal prodomain has no impact on the interactions between caspase-7 and XIAP (Chai et al., 2001). Thus, the N-terminal prodomain is dispensable for the activation of procaspase-7 or the activity of mature caspase-7.

The Loop-Bundle Is Indispensable for Substrate Binding and Catalysis

Compared to the closed conformation in the procaspase-7 zymogen, the L2′ loop in the inhibitor-bound caspase-7 is flipped 180°, existing in an open conformation and stabilizing the active site loops L2 and L4 (Figure 2). This structural observation demonstrates that the loop-bundle is important for the binding of inhibitors/substrates and the catalytic activity of caspase-7.

To confirm this conclusion, we generated three caspase-7 variants (Figure 3A), each of which contains an invariant large subunit (residues 51–198) and a distinct small subunit. This was achieved by coexpression of the large subunit in one vector and the small subunit in another compatible vector in bacteria (see Experimental Procedures). Thus, these caspase-7 variants represent their "cleaved" or "active" form. The only difference is that, relative to the wild-type (wt) caspase-7, the ΔS and ΔL variants contain deletion of residues 199–205 and 199–215, respectively (Figure 3A). Since the removal of residues 212–215 eliminates the formation of the loop-bundle, caspase-7 (ΔL) is expected to exhibit decreased binding efficiency for inhibitors/substrates and decreased catalysis. In contrast, the caspase-7 (ΔS) variant is expected to behave like the wt caspase-7.

First, we examined the ability of these caspase-7 variants to interact with the BIR2 domain (residues 124–240) of XIAP, which potently inhibits caspase-7 (Chai et al., 2001; Huang et al., 2001). As expected, both the wt caspase-7 and the ΔS variant formed a stable complex with a fusion protein between XIAP-BIR2 and glutathione S-transferase (GST) (Figure 3B, lanes 2 and 8). In sharp contrast, the ΔL variant was unable to bind XIAP-BIR2 (Figure 3B, lane 4). As a control, we also show that the procaspase-7 zymogen was unable to form a stable complex with XIAP-BIR2 (Figure 3B, lane 6), presumably due to the closed conformation of the L2′ loop.

Next, we examined the catalytic activity of these caspase-7 variants, using procaspase-9 as a substrate (Figure 3C). Caspase-7 is able to cleave after residue Asp330

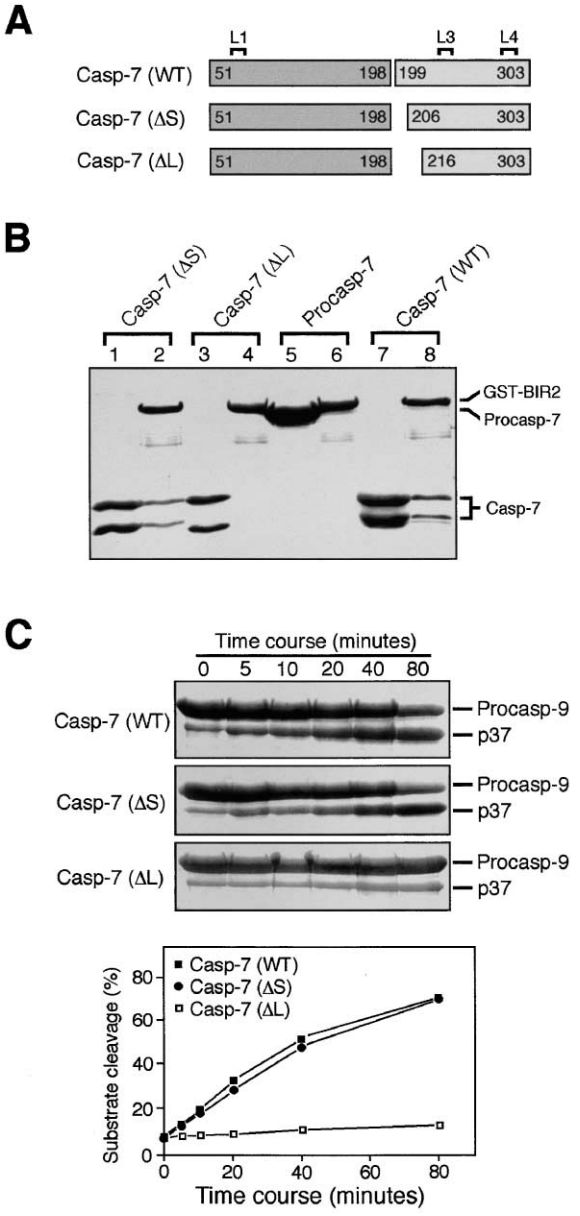

Figure 3. The Formation of the Loop-Bundle Is Indispensable to Substrate/Inhibitor Binding and Catalysis for Caspase-7

(A) Schematic diagram of three caspase-7 variants. Using a coexpression strategy, these proteins were produced in their "cleaved" form (see Experimental Procedures for details).

(B) Interactions between XIAP-BIR2 (residues 124–240) and the three caspase-7 variants. The interaction was examined by GST-mediated pull-down assays (see Experimental Procedures for details). For each caspase-7 variant, the left and right lanes indicate the input protein and the final complex, respectively. The molecular weight of procaspase-7 (lane 5) is 3 kDa smaller than that of GST-BIR2.

(C) A time course of procaspase-9 cleavage by the three caspase-7 variants. p37 represents the cleaved product. A small fraction (~7%) of the substrate procaspase-9 (C287A) was partially cleaved during purification, as indicated in the first lanes of the SDS-PAGE gels (0 min). The extent of cleavage is also plotted as a function of time in the lower panel for all three caspase-7 variants.

in procaspase-9, producing a p37 large subunit and a p10 small subunit. To prevent autocleavage, we mutated the catalytic residue Cys286 to Ala in the full-length

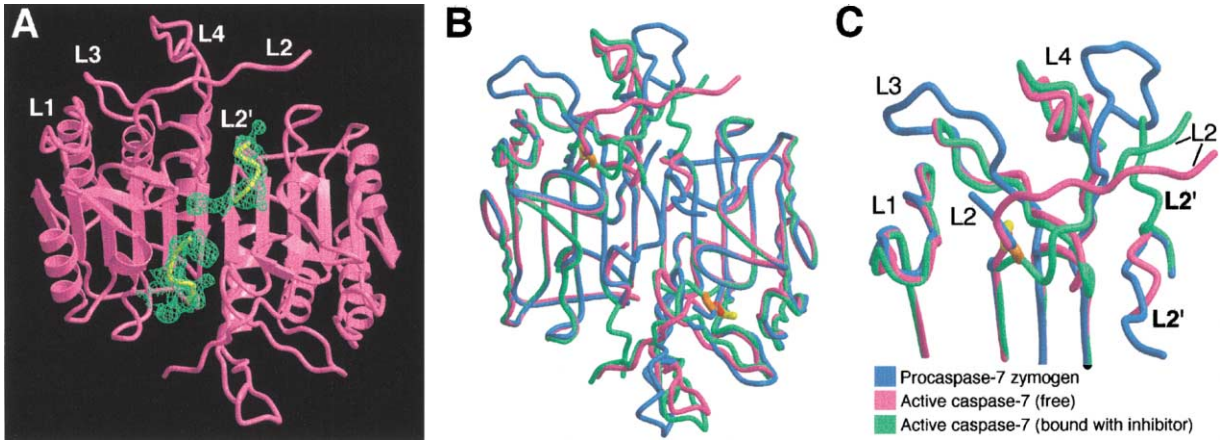

Figure 4. Structural Comparison of the Procaspase-7 Zymogen and the Isolated Active Caspase-7 without any Bound Cofactors

(A) Overall structure of the active caspase-7 without bound cofactors. The structure is shown in pink, with the N termini of the small subunits highlighted in yellow. The electron density (omit map) surrounding these regions, shown at 2.5 σ, was calculated by simulated annealing using CNS (Brunger et al., 1998). The four loops that define the catalytic groove are indicated.

(B) Superposition of the active caspase-7 without bound cofactors (pink), the procaspase-7 zymogen (blue), and the active caspase-7 (green) bound with an XIAP fragment. For clarity, the XIAP fragment is not shown.

(C) Closeup comparison of the four loops that define the catalytic cleft. Coloring scheme is the same as (B). Compared to a closed conformation in the procaspase-7 zymogen and the isolated active caspase-7, the L2′ loop switches to an open conformation in the inhibitor-bound caspase-7.

procaspase-9 (residues 1–416) and purified the resulting protein to homogeneity. Equal amounts of the caspase-7 variants were incubated with the procaspase-9 (C286A) substrate; the cleavage efficiency was monitored by SDS-PAGE and Coomassie staining (Figure 3C). In agreement with the binding results (Figure 3B), caspase-7 (ΔS) displayed the same level of catalytic activity as the wt protein, whereas caspase-7 (ΔL) was only marginally active (Figure 3C).

Structure of an Isolated Active Caspase-7

To further investigate the mechanisms of caspase-7 activation, we crystallized the active caspase-7 free from any bound inhibitors and determined its structure at 2.6 Å resolution (Figure 4A and Table 1). The space group for the crystals of this caspase-7 is $P3_221$, the same as that for the procaspase-7 zymogen and that for the active caspase-7 bound with a peptide inhibitor (Chai et al., 2001; Huang et al., 2001). This facilitates comparisons among the three structures, as they share the same set of crystal lattice contacts.

Surprisingly, although the isolated active caspase-7 is somewhat more similar to the inhibitor-bound caspase-7 than the procaspase-7 zymogen, significant structural differences remain (Figure 4B). Most strikingly, despite cleavage after Asp198, the loop L2′ in the isolated caspase-7 still exists in the closed conformation, mimicking the procaspase-7 zymogen (Figure 4A). Consequently, the loop-bundle is not properly assembled and the catalytic cleft is not well defined (Figure 4C). Nevertheless, the L3 and L4 loops in the isolated caspase-7 have moved closer to their productive conformation after the activation cleavage (Figure 4).

This unanticipated finding indicates that the isolated active caspase-7 adopts a conformation intermediate between that of the zymogen and that of the inhibitor-bound caspase-7. Thus, inhibitor/substrate binding triggers a 180° flipping of the L2′ loop in the active caspase-7, changing its closed conformation in the isolated caspase-7 to an open form in the loop-bundle in the inhibitor-bound caspase-7. This movement is apparently prohibited in the procaspase-7 zymogen prior to cleavage at Asp198. Therefore, the procaspase-7 zymogen is unable to interact with substrates or inhibitors (Figure 3B).

Thus, the interdomain cleavage initiates a conformational change in the active site loops and primes caspase-7 for substrate/inhibitor binding, and the actual binding by substrates/inhibitors completes the conformational change to a fully productive state (Figure 5). The intrinsic conformational flexibility of the active site loops constitutes an important consideration for the design and screening of caspase inhibitors.

Discussion

Our structural analyses demonstrate that the conformation of the active site loops of procaspase-7 zymogen, particularly that of the L2′ and L2 loops, is ineffective for substrate/inhibitor binding. The underlying restraint is the covalent linkage in the interdomain region that precludes the formation of a productive conformation (Figure 5). Cleavage after Asp198 leads to some rearrangement in loops L2, L3, and L4 (Figure 4C), which adopt conformations that are more similar to those in the inhibitor-bound caspase-7 (Figure 5). The critical L2′ loop, however, retains a closed conformation, presumably a lower energy state. Inhibitor/substrate binding removes the energy barrier and induces the flipping of the L2′ loop and subsequent formation of a loop-bundle, stabilizing the inhibitor/substrate-bound conformation (Figure 5). Consequently, the four active site loops, L1, L2, L3, and L4, as well as the critical L2′ loop, appear to be well-ordered and fairly rigid, as judged by their

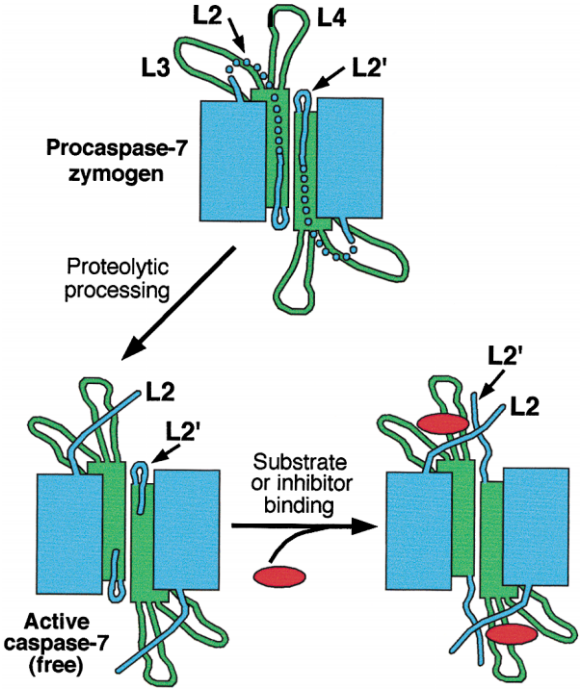

Figure 5. Schematic Diagram of Caspase Activation and Substrate/Inhibitor Binding

The active site loops in procaspase-7 zymogen are in an unproductive conformation for catalysis. The contiguous interdomain loop in the procaspase-7 zymogen locks the interdomain loop in a closed conformation and precludes a conformational change that must accompany substrate/inhibitor binding. The proteolytic cleavage after Asp198 rearranges the active site loops and produces a free N terminus in the small subunit (L2′). These changes ready the active caspase-7 for substrate/inhibitor binding, which further induces a drastic conformational switch.

low temperature factors in the crystals. This gives the incorrect impression that the catalytic cleft may be preformed prior to inhibitor/substrate binding. In comparison, the active site loops in the procaspase-7 zymogen and the isolated active caspase-7 are not stabilized by the inhibitor/substrate binding-induced interactions and thus exhibit much greater conformational flexibility. The intrinsic conformational flexibility of the active site loops is essential to the catalytic activity of caspase-7.

In this mechanism, the ability of loop L2′ to move freely in response to inhibitor/substrate binding is a decisive feature. In caspase-7, this ability is acquired through proteolytic cleavage after Asp198. Because L2′ is at the N terminus of the small subunit, our findings predict that inverting the order of primary sequences of the large and small subunits might constitutively activate caspase-7. Although it remains to be formally proved for caspase-7, this prediction has been confirmed for two other human effector caspases, caspase-3 and -6 (Srinivasula et al., 1998b) and the *Drosophila* caspase drICE (Wang et al., 1999). Moreover, the catalytic activity of this reversed caspase-3 does not require the interdomain cleavage (Srinivasula et al., 1998b), presumably because the L2′ loop is free to adopt the open conformation in response to substrate binding.

In a recent report, an acidic tripeptide (Asp179-Asp180-Asp181) immediately after the interdomain cleavage site was implicated in the maintenance of procaspase-3 dormancy (Roy et al., 2001). The underlying mechanism was attributed to multiple ionic interactions (Roy et al., 2001). The corresponding residues for this tripeptide are conserved in caspase-7 (Asp204-Thr205-Asp206) (Figure 2D) and are visible in the electron density map. However, these residues are not involved in multiple ionic interactions in the crystal structure. In our own experience, the reasons for increased proenzyme dormancy are hard to pinpoint, particularly in the absence of relevant structural information. For example, the missense mutation D168A in procaspase-7 significantly increased its proenzyme dormancy (our unpublished data). Our structural studies, together with published evidence (Srinivasula et al., 1998a, 1998b; Wang et al., 1999), unambiguously demonstrate that the proenzyme dormancy of caspases is predominantly due to the covalent linkage between the large and the small subunits.

The activation mechanism of procaspase-7 bears an interesting analogy to the serpin-mediated inhibition of serine proteases. A prototypical serpin, α1-antitrypsin, inhibits the catalytic activity of trypsin by covalently trapping trypsin through an ester linkage; the serpin-bound protease undergoes dramatic conformational change and exhibits a deformed catalytic site (Huntington et al., 2000). Similarly, the procaspase-7 zymogen is also trapped in an inactive state by a covalent linkage in the interdomain, which also produces a deformed catalytic cleft (Figure 1).

The quaternary structure of caspase-7 comprises two closely associated heterodimers, with each heterodimer consisting of a large and a small subunit. Because the interdomain sequence is inherently flexible and disordered in solution, two contrasting models of interdomain linkage have been proposed based on previous structural studies on caspase-1 and -3 (Rotonda et al., 1996; Walker et al., 1994; Wilson et al., 1994). It was suggested that a drastic conformational change in the L2′ loop would have to take place to account for the model in which the adjacent large and small subunits are derived from the same polypeptide chain. Indeed, relative to the inhibitor-bound caspase-7, the L2′ loop in the uncleaved procaspase-7 zymogen is flipped by 180° (Figures 1A and 5). This observation strongly suggests that each heterodimer is derived from a single contiguous polypeptide, a conclusion further supported by recent in vitro studies using recombinant proteins (Srinivasula et al., 1998a, 1998b). Moreover, the directions of the L2 and L2′ loops in procaspase-7 make the other model, in which the interdomain sequence would have to adopt severely restrained conformation, highly unlikely.

In summary, our structural analyses reveal the mechanisms of caspase-7 activation and the induced-fit nature of substrate/inhibitor binding for caspase-7. These conclusions are likely applicable to other caspases and should serve a general framework for the understanding of caspases.

Experimental Procedures

Protein Preparation

All constructs were generated using a standard PCR-based cloning strategy, and the identities of individual clones were verified through double-stranded plasmid sequencing. To avoid autocatalytic cleav-

age in bacteria, the full-length procaspase-7 zymogen (residues 1–303) contains a missense mutation (C186A) in the active site residue Cys186. This procaspase-7 zymogen and procaspase-9 (C286A) were overexpressed in *Escherichia coli* strain BL21(DE3) as a C-terminally 6-Histidine-tagged protein using a pET-21b vector (Novagen). The soluble fraction of the recombinant protein in the *E. coli* lysate was purified using a Ni-NTA (Qiagen) column, and further fractionated by anion-exchange (Source-15Q, Pharmacia) and gel-filtration chromatography (Superdex-200, Pharmacia). Recombinant active caspase-7 and XIAP-BIR2 were overexpressed and purified as described (Chai et al., 2001).

For the three caspase-7 variants (Figure 3A), the large and small subunits were cloned into the vectors pET3d (Amp^R, Novagen) and pBB75 (Kan^R) (Batchelor et al., 1998), respectively, and coexpressed in *E. coli* strain BL21(DE3). A 6-Histidine tag was fused C-terminally to the small subunit to facilitate purification.

Crystallization and Data Collection

Crystals were grown by the hanging-drop vapor-diffusion method by mixing protein with an equal volume of reservoir solution. For the procaspase-7 zymogen, the well buffer contains 100 mM Citrate (pH 5.8), 1.0 M lithium sulfate, and 1.0 M sodium chloride. For the active caspase-7, the well buffer contains 10% PEG 4000 and 2.0 M sodium chloride. Showers of small crystals appeared overnight in both cases. Macroseeding yielded crystals with a typical size of $0.2 \times 0.2 \times 0.4$ mm^3 over a period of 6–7 days. The crystals for both the zymogen and the active caspase-7 are in the primitive trigonal space group $P3_221$, and contain two molecules in each asymmetric unit. The unit cell dimensions of the active caspase-7, a = b = 88.9 Å and c = 186.2 Å, are very similar to those of the active caspase-7 bound with an XIAP fragment (a = b = 89.6 Å, c = 185.5 Å). The unit cell dimensions of the procaspase-7 zymogen, a = b = 91.2 Å and c = 182.5 Å, are somewhat different. Diffraction data were collected at the National Synchrotron Light Source beamline X25 in the Brookhaven National Laboratory. For the frozen data sets, crystals were equilibrated in a cryoprotectant buffer containing well buffer plus 20% glycerol, and were flash frozen in a −170°C nitrogen stream. All data sets were processed using the software Denzo and Scalepack (Otwinowski and Minor, 1997).

Structure Determination

Both structures were determined by molecular replacement, using the software AMoRe (Navaza, 1994). The atomic coordinates of active caspase-7 (PDB code 1I51) were used for rotational search against a 15–3.2 Å data set. The top solutions from the rotational search were individually used for a subsequent translational search, which yielded the correct solutions with high correlation factors. Refinement was performed using the program CNS (Brunger et al., 1998). For both active caspase-7 and the zymogen, electron density surrounding the catalytic cleft was carefully examined. A model was built with the program O (Jones et al., 1991) and refined further by simulated annealing using the program CNS. The final refined atomic model for the active caspase-7 contains residues 58–196 and 212–303, and 111 ordered water molecules at 2.6 Å resolution. The final refined atomic model for the procaspase-7 zymogen contains residues 56–188 and 208–303 for one heterodimer, and residues 56–189 and 204–303 for the other heterodimer, at 2.7 Å resolution.

Caspase-7 Assay

The reaction was performed at 37°C under the following buffer conditions: 25 mM HEPES (pH 7.5), 100 mM KCl, and 1 mM dithiothreitol (DTT). The substrate (procaspase-9, C286A) concentration was approximately 200 μM. Caspase-7 variants were diluted to the same concentration (0.5 μM) with the assay buffer. Reactions were stopped with the addition of an equal volume 2X SDS loading buffer and boiled for three minutes. The samples were applied to SDS-PAGE and the results were visualized by Coomassie staining.

In Vitro Interaction Assay

Interaction between caspase-7 variants and GST-XIAP-BIR2 was examined by GST-mediated pull-down assays. Approximately 0.4 mg of recombinant XIAP-BIR2 was bound to 200 μl of glutathione resin as a GST-fusion protein and incubated with excess amounts of caspase-7 variants at room temperature. After extensive washing with an assay buffer containing 25 mM Tris (pH 8.0), 150 mM NaCl, and 2 mM dithiothreitol (DTT), the complex was eluted with 5 mM reduced glutathione and visualized by SDS-polyacrylamide gel electrophoresis (SDS-PAGE) with Coomassie staining.

Acknowledgments

We thank Michael Becker at the NSLS-X25 beamline for assistance, F. Hughson for critically reading the manuscript, and N. Hunt for administrative assistance. This research was supported by NIH grants CA90269 (Y.S.) and AG14357 (E.A.). Y.S. is a Searle Scholar and a Rita Allen Scholar. S.M.S is a special fellow of the Leukemia and Lymphoma Society.

Received September 11, 2001; revised September 28, 2001.

References

Batchelor, A.H., Piper, D.E., de la Brousse, F.C., McKnight, S.L., and Wolberger, C. (1998). The structure of GABPalpha/beta: an ETS domain-ankyrin repeat heterodimer bound to DNA. Science *279*, 1037–1941.

Blanchard, H., Kodandapani, L., Mittl, P.R.E., Di Marco, S., Krebs, J.K., Wu, J.C., Tomaselli, K.J., and Grutter, M.G. (1999). The three dimersional structure of caspase-8: an initiator enzyme in apoptosis. Structure *7*, 1125–1133.

Brunger, A.T., Adams, P.D., Clore, G.M., Delano, W.L., Gros, P., Grosse-Kunstleve, R.W., Jiang, J.S., Kuszewski, J., Nilges, M., Pannu, N.S., et al. (1998). Crystallography and NMR system: A new software suite for macromolecular structure determination. Acta Crystallogr. D *54*, 905–921.

Budihardjo, I., Oliver, H., Lutter, M., Luo, X., and Wang, X. (1999). Biochemical pathways of caspase activation during apoptosis. Annu. Rev. Cell Dev. Biol. *15*, 269–290.

Cerreti, D.P., Kozlosky, C.J., Mosley, B., Nelson, N., Van Ness, K., Greenstreet, T.A., March, C.J., Kronheim, S.R., Druck, T., Cannizzaro, L.A., et al. (1992). Molecular cloning of the interleukin-1 beta converting enzyme. Science *256*, 97–100.

Chai, J., Shiozaki, E., Srinivasula, S.M., Wu, Q., Datta, P., Alnemri, E.S., and Shi, Y. (2001). Structural basis of caspase-7 inhibiton by XIAP. Cell *104*, 769–780.

Cheng, Y., Deshmukh, M., D'Costa, A., Demaro, J.A., Gidday, J.M., Shah, A., Sun, Y., Jacquin, M.F., Johnson, E.M., and Holtzman, D.M. (1998). Caspase inhibitor affords neuroprotection with delayed administration in a rat model of neonatal hypoxic-ischemic brain injury. J. Clin. Invest. *101*, 1992–1999.

Endres, M., Namura, S., Shimizu-Sasamata, M., Waeber, C., Zhang, L., Gomez-Isla, T., Hyman, B.T., and Moskowitz, M.A. (1998). Attention of delayed neuronal death after mild focal ischemia in mice by inhibition of the caspase family. J. Cereb. Blood Flow Metab. *18*, 238–247.

Fernandes-Alnemri, T., Takahashi, A., Armstrong, R., Krebs, J., Fritz, L., Tomaselli, K.J., Wang, L., Yu, Z., Croce, C.M., Salvesen, G., et al. (1995). Mch3, a novel human apoptotic cysteine protease highly related to CPP32. Cancer Res. *55*, 6045–6052.

Horvitz, H.R. (1999). Genetic control of programmed cell death in the nematode Caenorhabditis elegans. Cancer Res. *59*, 1701–1706.

Huang, Y., Park, Y.C., Rich, R.L., Segal, D., Myszka, D.G., and Wu, H. (2001). Structural basis of caspase inhibition by XIAP: Differential roles of the linker versus the BIR domain. Cell *104*, 781–790.

Huntington, J.A., Read, R.J., and Carrell, R.W. (2000). Structure of a serpin-protease complex shows inhibition by deformation. Nature *407*, 923–926.

Jacobson, M.D., Weil, M., and Raff, M.C. (1997). Programmed cell death in animal development. Cell *88*, 347–354.

Jones, T.A., Zou, J.-Y., Cowan, S.W., and Kjeldgaard, M. (1991). Improved methods for building protein models in electron density maps and the location of errors in these models. Acta Crystallogr. *A47*, 110–119.

Klaulis, P.J. (1991). Molscript: a program to produce both detailed and schematic plots of protein structures. J. Appl. Crystallogr. *24*, 946–950.

Mittl, P.R., Di Marco, S., Krebs, J.F., Bai, X., Karanewsky, D.S., Priestle, J.P., Tomaselli, K.J., and Grutter, M.G. (1997). Structure of recombinant human CPP32 in complex with the tetrapeptide acetyl-Asp-Val-Ala-Asp fluoromethyl ketone. J. Biol. Chem. *272*, 6539–6547.

Navaza, J. (1994). AMoRe and automated package for molecular replacement. Acta Crystallogr. *A50*, 157–163.

Nicholls, A., Sharp, K.A., and Honig, B. (1991). Protein folding and association: insights from the interfacial and thermodynamic properties of hydrocarbons. Proteins *11*, 281–296.

Otwinowski, Z., and Minor, W. (1997). Processing of X-ray diffraction data collected in oscillation mode. Methods Enzymol. *276*, 307–326.

Riedl, S.J., Renatus, M., Schwarzenbacher, R., Zhou, Q., Sun, C., Fesik, S.W., Liddington, R.C., and Salvesen, G.S. (2001). Structural basis for the inhibition of caspase-3 by XIAP. Cell *104*, 791–800.

Rodriguez, I., Matsuura, K., Ody, C., Nagata, S., and Vassalli, P. (1996). Systemic injection of a tripeptide inhibits the intracellular activation of CPP32-like proteases in vivo and fully protects mice against Fas-mediated fulminant liver destrcution and death. J. Exp. Med. *184*, 2067–2072.

Rotonda, J., Nicholson, D.W., Fazil, K.M., Gallant, M., Gareau, Y., Labelle, M., Peterson, E.P., Rasper, D.M., Ruel, R., Vaillancourt, J.P., et al. (1996). The three-dimensional structure of apopain/CPP32, a key mediator of apoptosis. Nature-Struct. Biol. *3*, 619–625.

Roy, S., Bayly, C.I., Gareau, Y., Houtzager, V.M., Kargman, S., Keen, S.L.C., Rowland, K., Seiden, I.M., Thornberry, N.A., and Nicholson, D.W. (2001). Maintenance of caspase-3 proenzyme dormancy by an intrinsic "safety catch" regulatory tripeptide. Proc. Natl. Acad. Sci. USA *98*, 6132–6137.

Shi, Y. (2001). A structural view of mitochondria-mediated apoptosis. Nature Struct. Biol. *8*, 394–401.

Srinivasula, S.M., Ahmad, M., Fernandes-Alnemri, T., and Alnemri, E.S. (1998a). Autoactivation of procaspase-9 by Apaf-1-mediated oligomerization. Mol. Cell *1*, 949–957.

Srinivasula, S.M., Ahmad, M., MacFarlane, M., Luo, Z., Huang, Z., Fernandes-Alnemri, T., and Alnemri, E.S. (1998b). Generation of constitutively active recombinant caspase-3 and -6 by rearrangeement of their subunits. J. Biol. Chem. *273*, 10107–10111.

Srinivasula, S.M., Saleh, A., Hedge, R., Datta, P., Shiozaki, E., Chai, J., Robbins, P.D., Fernandes-Alnemri, T., Shi, Y., and Alnemri, E.S. (2001). A conserved XIAP-interaction motif in caspase-9 and Smac/DIABLO mediates opposing effects on caspase activity and apoptosis. Nature *409*, 112–116.

Steller, H. (1995). Mechanisms and genes of cellular suicide. Science *267*, 1445–1449.

Stennicke, H.R., Deveraux, Q.L., Humke, E.W., Reed, J.C., Dixit, V.M., and Salvesen, G.S. (1999). Caspase-9 can be activated without proteolytic processing. J. Biol. Chem. *274*, 8359–8362.

Thompson, C.B. (1995). Apoptosis in the pathogenesis and treatment of disease. Science *267*, 1456–1462.

Thornberry, N.A., Bull, H.G., Calaycay, J.R., Chapman, K.T., Howard, A.D., Kostura, M.J., Miller, D.K., Molineaux, S.M., Weidner, J.R., Aunins, J., et al. (1992). A novel heterodimeric cysteine protease is required for interleukin-1 beta processing in monocytes. Nature *356*, 768–774.

Thornberry, N.A., and Lazebnik, Y. (1998). Caspases: Enemies within. Science *281*, 1312–1316.

Walker, N.P., Talanian, R.V., Brady, K.D., Dang, L.C., Bump, N.J., Ferenz, C.R., Franklin, S., Ghayur, T., Hackett, M.C., and Hammill, L.D. (1994). Crystal structure of the cysteine protease interleukin-1b-converting enzyme: a (p20/p10)2 homodimer. Cell *78*, 343–352.

Wang, S., Hawkins, C., Yoo, S., Muller, H.-A., and Hay, B. (1999). The Drosophila caspase inhibitor DIAP1 is essential for cell survival and is negatively regulated by HID. Cell *98*, 453–463.

Watt, W., Koeplinger, K.A., Mildner, A.M., Heinrikson, R.L., Tomasselli, A.G., and Watenpaugh, K.D. (1999). The atomic-resolution structure of human caspase-8, a key activator of apoptosis. Structure *7*, 1135–1143.

Wei, Y., Fox, T., Chambers, S.P., Sintchak, J.-A., Coll, J.T., Golec, J.M.C., Swenson, L., Wilson, K.P., and Charifson, P.S. (2000). The structures of caspases-1, -3, -7 and -8 reveal the basis for substrate and inhibitor selectivity. Chem. Biol. *7*, 423–432.

Wilson, K.P., Black, J.-A., Thomson, J.A., Kim, E.E., Griffith, J.P., Navia, M.A., Murcko, M.A., Chambers, S.P., Aldape, R.A., Raybuck, S.A., and Livingston, D.J. (1994). Structure and mechanism of interleukin-1b converting enzyme. Nature *370*, 270–275.

Yakovlev, A.G., Knoblach, S.M., Fan, L., Fox, G.B., Goodnight, R., and Faden, A.I. (1997). Activation of CPP32-like caspases contributes to neuronal apoptosis and neurological dysfunction after traumatic brain injury. J. Neurosci. *17*, 7415–7424.

Yuan, J., and Yankner, B.A. (2000). Apoptosis in the nervous system. Nature *407*, 802–809.

Accession Numbers

Atomic coordinates for the procaspase-7 zymogen and the active caspase-7 have been deposited in the Protein Data Bank under accession numbers 1K88 and 1K86, respectively.